Transport in Stochastic Fibrous Networks

X. Cheng

A. M. Sastry

B. E. Layton

Department of Mechanical Engineering
and Applied Mechanics,
The University of Michigan,
Ann Arbor, MI 48109-2125

Some fundamental issues concerning the design and performance of stochastic porous structures are examined, stemming from application of advanced fibrous electrode substrates in NiMH automotive cells. These electrodes must resist corrosion and local failures under hundreds of charge/discharge cycles. Such fibrous materials can be effectively used as substrates for chemical reactions because of their combinations of high surface area and high conductivity. Key questions concerning the relationships among connectivity and conductivity, scale and variability in material response are addressed. Two techniques are developed and compared for use in predicting these materials' conductivity. The first approach uses a statistical technique in conjunction with an adaptation of classic micromechanical models. The second approach uses the statistical generation technique, followed by an exact calculation of 2D network conductivity. The two techniques are compared with one another and with classic results. Several important conclusions about the design of these materials are presented, including the importance of use of fibers with aspect ratios greater than at least 50, the weak effect of moderate alignment for unidirectional conductivity, and the weak power-law behavior of conductivity versus volume fraction over the range of possible behaviors.
[DOI: 10.1115/1.1322357]

I Introduction: Transport in Battery Substrates

Recently-developed substrate materials for production of positive electrodes for NiMH (nickel-metal hydride) batteries are comprised of two or more phases and generally have high porosity. In construction of a cell, these open networks of nickel fibers and/or particles are packed with an active material, whose constituents are depleted and replenished during the cell reaction. The substrate is an open network, which acts in the cell as a grid to both contain active material and enhance conduction in the positive plate. An example of this type of material is shown in Fig. 1. Maintenance of high conductivity (achieved through both high nickel mass and sufficient surface area) of the substrate is essential to proper function of the cell. Conversely, low substrate mass is desirable in the cell, since high energy densities require low total cell weight. For these reasons, careful design of low-cost substrates requires precise prediction of substrate conductivity, based on microstructure. Low-cost production techniques [1,2] are available to produce these materials, but each induces inherent variability in the material. The lowest-cost production methods are papermaking-type processes, which result in materials of nearly random architecture. Some control of fiber orientation can be achieved in this general class of materials, as has been done in the case of fibrous materials for use in preforming, in polymeric composites, but at sometimes significant cost penalty. Staple length and fiber diameter, however, can generally be selected easily.

One mechanism by which progressive damage occurs in the Ni/MH substrate is swelling in the positive plate due to the formation of the γ-NiOOH phase, which is of lower density than the β-$Ni(OH)_2$. This γ-phase is largely unrecoverable in the electrochemical reaction. Accumulation of this compound in the positive plate (particularly during overcharge) leads to fatigue upon charge/discharge cycles of the electrodes, which limits cell performance [3,4]. The prime effect of this mechanical damage is in the loss of conductivity in the positive plate. Another mechanism for significantly reduced conductivity in transport behavior is a gradual deposition of nickel onto the main network from smaller, interconnecting particulate outcroppings on the fibers [5,6].

Dry conductivity of the substrate (conductivity of the substrate before it is loaded with active material) has been shown to be correlated with superior electrode performance. It also provides a convenient proof test for manufacturers. Thus, the key goals of the present work are

1 *to accurately predict electrical conductivity* of these random, porous structures, as a function of readily controllable microstructural features,

2 *to accurately predict the variability in the measured conductivities* (resistivities) in as-manufactured materials, so that measurement of conductivity (resistivity) can be used as a proof-test of material quality, and also because of the dependence of performance variability upon material variability, and

3 *to assess the benefits of precise placement of fibers* as square grids or hexagonal foams, in comparison to placing fibers in statistically random orientations.

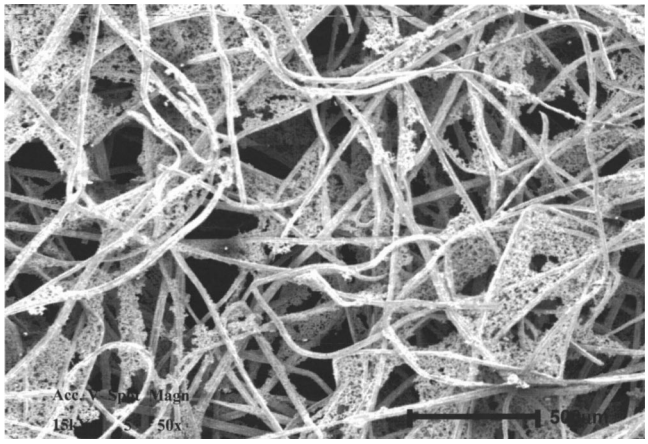

Fig. 1 Scanning electron micrograph of a nickel substrate (positive plate) used in the Ni/MH cell. The material pictured is comprised of nickel fibers, sinter bonded into a network of approximately 97% porosity (National Standard, Advanced Fiber Substrate material).

Contributed by the Materials Division for publication in the JOURNAL OF ENGINEERING MATERIALS AND TECHNOLOGY. Manuscript received by the Materials Division April 14, 1999; revised manuscript received July 31, 2000. Associate Technical Editor: J. W. Ju.

The present approaches developed to address these issues are compared with work in effective medium theories, and in network percolation.

Statistical Description of, and Determination of Percolation in Fibrous Media. Broadbent and Hammersly [7] were probably the first workers to formally study percolation thresholds, introducing lattice models for fluid flow through statistically random media. Later, Kallmes and Corte [8] addressed the problem of percolation in fibrous networks by developing basic relationships among number of fibers, bonds, segment lengths and areal density, based on probability and trigonometry, as

$$N_c = \frac{1}{2}(1+e^{-H})\frac{N_f^2\lambda^2}{A}\left(\frac{1}{\pi}-\frac{e^2\pi}{6}\right) \tag{1}$$

where

N_c: number of bonds (fiber crossings)
N_f: number of fibers
$H = N_f\lambda\omega/A$
A: area
λ: fiber length
ω: fiber width
e: eccentricity of orientation

and the distribution function for the fibers (2D) is represented by the first two terms in a Fourier series as

$$\Theta(\theta) = 1/\pi + e\cos 2\pi \tag{2}$$

For a statistically random material, $e=0$. Thus the resulting number of crossings for a fibrous network, where fibers have statistically random orientation (and centers are located via a 2D Poisson point process), is given by

$$N_c = \frac{(1+e^{-H})N_f^2\lambda^2}{2\pi A} \tag{3}$$

This model [1,9] represents a simple, closed-form solution for bond density in a 2D array of fibers, and can be used in conjunction with semi-empirical approaches to predict effective conductivity. One early and influential example of such a semi-empirical approach was put forward by Kirkpatrick [10], wherein percolation thresholds were identified based on ''bond'' or ''lattice'' percolation; in simulation results for simple 2D and 3D cubic lattices, a power law form was observed to related conductivity and p (bond fraction), as

$$G(p) \propto (p-p_c)^t \tag{4}$$

The values of t and p_c, the exponent and critical (percolation) bond fraction were postulated to be determined by structure. This power law relation was also postulated for use in determining critical volume fraction, using the same exponent t, as

$$G(\nu) \propto (V-V_c)^t \tag{5}$$

where V is conducting volume fraction and V_c is the critical volume fraction. The exponent t, as determined for a particular type of microstructure, can be used to empirically fit a power-law increase in conductivity with added material. Stauffer [11], for example, proposed use of universal values of 1.3 (2D) and 1.7 (3D) for t.

Classic work by Pike and Seager [12,13] focused specifically on fibrous structures. They identified percolation thresholds in 1-D fibers via Monte Carlo methods, and compared these with existing analytical solutions for a few particular cases. Balberg and Binenbaum [14,15] evaluated effects including aspect ratio of fibers, anisotropy in networks, and distributions of lengths. One general result of the latter work was that anisotropic systems were found to have higher percolation thresholds than fully isotropic (random) systems, per an analytic result. In all cases, unit cells for simulations were generated by placement of fibers in a cell, with the centerpoints located by Poisson point processes (2D). Fibers extending beyond the boundaries of the cells were apparently truncated. Work on conduction in short fiber composites [16] has been similarly interested in identification of percolation. Some published work using Delaunay networks has also shed insight into the conduction of fibrous materials [17,18]; these have focused particularly on effect of scale in solution. As such, they offer another way of representing 1D fibers, but in a triangulated network which similarly does not take direct account of material ''wastage'' as it occurs in real materials (i.e., fiber ends which do not provide connectivity in the network but nonetheless contribute to overall mass).

Closed-Form Effective Media Approaches. There is a large body of literature available on the conductivity of model microstructures comprised of two or more phases (see, for example, the review of Meredith and Tobias [19] for solutions in electrostatics, and Batchelor [20] for generalized media). These solutions can be applied to the current case of a porous fibrous medium if one phase of a heterogeneous media studied is assumed to be nonconductive. A general governing equation for such models may be written as Laplace's equation

$$\nabla^2 U = 0 \tag{6}$$

where U is electronic potential. Compatibility conditions (e.g., electric flux) are enforced at the phase boundaries. In the case of ''high-contrast'' materials, i.e., materials wherein the phases have very different conductivities great simplification is achieved. Several of these approaches result in the same general solution for effective conductivity or bulk modulus [21–23] as

$$K = \frac{(k_1+2k_2)-2f(k_2-k_1)}{(k_1+2k_2)+f(k_2-k_1)}k_2 \tag{7a}$$

where k_1 and k_2 are the conductivities of phases 1 and 2, f is the volume fraction of phase 1, and K is the conductivity of the heterogeneous medium. This, in turn, can be reduced to an expression for effective conductivity $\bar{K}$ (i.e., the conductivity of the porous medium normalized by the conductivity of the conductive phase, phase 2) as

$$\bar{K} = \frac{2f'}{3-f'} \tag{7b}$$

where f' is the conductivity of the conductive phase (i.e., $f'=1-f$), and the other phase is an insulator. In the fibrous materials under consideration, the conductive phase, comprised of the point-bonded fibers, is the continuum (''matrix'') phase, although it comprises a small total volume fraction of the material. Thus, in contrast to geometries studied in classic approaches, the continuum phase (fiber) has both small total volume fraction and high conductivity relative to the inclusion phase.

Regular Lattice Approaches. Several workers, particularly those working on foams, have developed relations for the effective properties of regular lattices, in both 2D and 3D [24,25]. In the present study, we are interested in comparison of stochastic structures with regular structures, in order to evaluate whether the higher inherent cost of regular microstructures is merited by improvement in conductivity. Two of these provide good comparisons. The first is the case of a square lattice comprised of rods, an orthotropic arrangement having conductivity along the fiber directions of

$$\frac{K_{\text{eff}}}{K_f} = \frac{V_f^{\text{Rod}}}{2} \tag{8}$$

The second is for a hexagonal array comprised of rods, which similarly has conductivity given by (8). The latter case is an isotropic arrangement. The optimal placement of fibers for conduction in a single direction would be of course a parallel arrangement of fibers, with axes aligned in the direction of current. The resulting conductivity in this case is simply

$$\frac{K_{\text{eff}}}{K_f} = V_f^{\text{Rod}} \tag{9}$$

which represents the upper bound on all fiber arrangements, for unidirectional conduction. The other two cases represent upper bounds for 2D conduction.

II Transport in Fibrous Media: Stochastic Approaches

Neither the statistical/percolation, nor regular lattice, nor effective medium approaches can adequately predict variances in conductivity. And, although there are theoretical bounds on conduction, of series and parallel resistors, they provide too wide a range of possible results to be practical, especially at the lower bound, where resistors in series have zero conductivity.

Present Approach: Network Generation. An alternative method for generating 2D stochastic fiber structures has been developed and is used in two new methods presented here. A complete illustration of the computational network generation approach is shown (Fig. 2). Fibers of a given staple length (relative to the unit cell dimension, and described hereafter as L/L_u) and orientation distribution function are placed randomly in a unit cell via random location of x- and y-coordinate of the centerpoints within the cell boundaries (Fig. 2(a)). Fiber ends lying outside the unit cell are ''wrapped'' back inside the cell, creating a periodic structure. Then, extraneous ends are numerically ''trimmed,'' for unidirectional current flow, i.e., all fiber ends and segments intersecting the sides of the cell transverse to current flow are eliminated (Fig. 2(b)). This eliminates unnecessary computation, and allows assessment of the volume of material conducting current. The use of periodic boundary conditions allows straightforward selection of properties which apply equally to the material as a whole, and to the unit cell, such as fiber volume fraction and average orientation. In the absence of use of periodic conditions, these parameters (volume fraction, orientation distribution function) change for each realization/simulation, depending upon how many fibers are ''cut off'' by the cell's boundaries. This process was automated in a computer program, and used to generate all networks studied here.

Connectivity in Network Structures. We define ''utilized volume fraction'' as the volume fraction of fibers for a reduced network in the case of unidirectional current flow. Fibers spanning the unit cell transverse to the direction of current (with direction chosen *a priori*) are eliminated, as in Fig. 2(b). Current direction is left-to-right. This eliminates some of the fiber segments which span the unit cell transverse to the flow direction, and is thus a conservative estimate of utilized volume fraction; this point is further discussed later. Figures 3, 4, and 5 show the results of simulations on microstructures containing several types of conductive fiber shapes. The first two plots show network characteristics for the case where $L = L_u$. Figures 3(a) and 3(b), give, respectively, the utilized volume fraction versus the initial volume fraction (averaged data from twenty simulations at each condition are shown); and the effective network conductivity versus number of bonds, over a range of aspect ratios ($L/D = 100, 50, 10$). Figures 4(a) and 4(b) give the corresponding results for staple lengths chosen to be 1.5 times the dimension of the unit cell (L/L_u

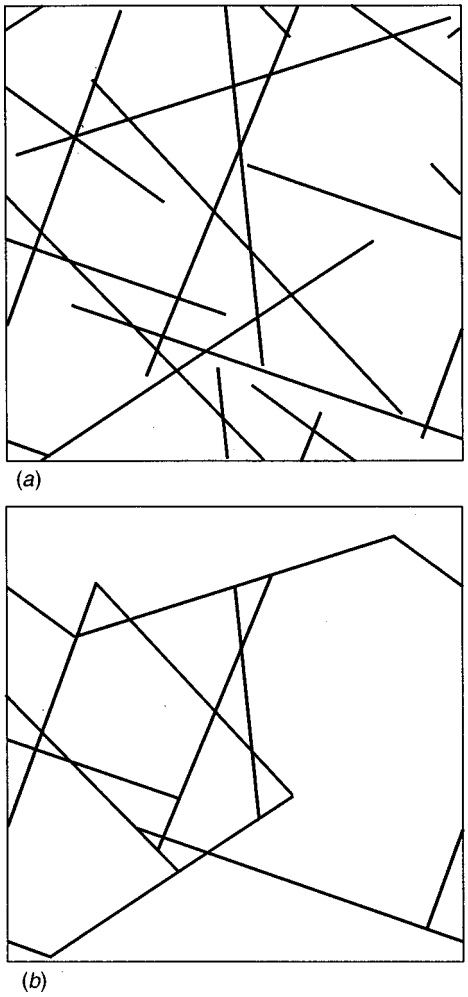

Fig. 2 Network generation approach (after Cheng et al. [5]). A stochastic array of 1D fibers (*a*) is modified to enforce periodicity, then nonconductive ends are removed to assess the effective volume fraction utilized for unidirectional conductivity (*b*)

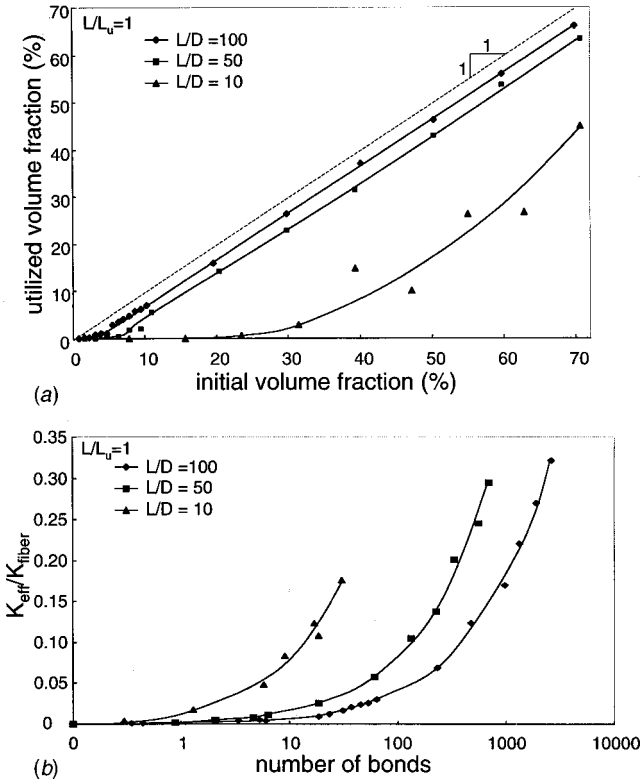

Fig. 3 (*a*) Utilized volume fraction versus original volume fraction, and (*b*) bond density, for various aspect ratios, for the case where the staple length is equal to the unit cell length. Twenty simulations were performed for each case; averaged data are shown.

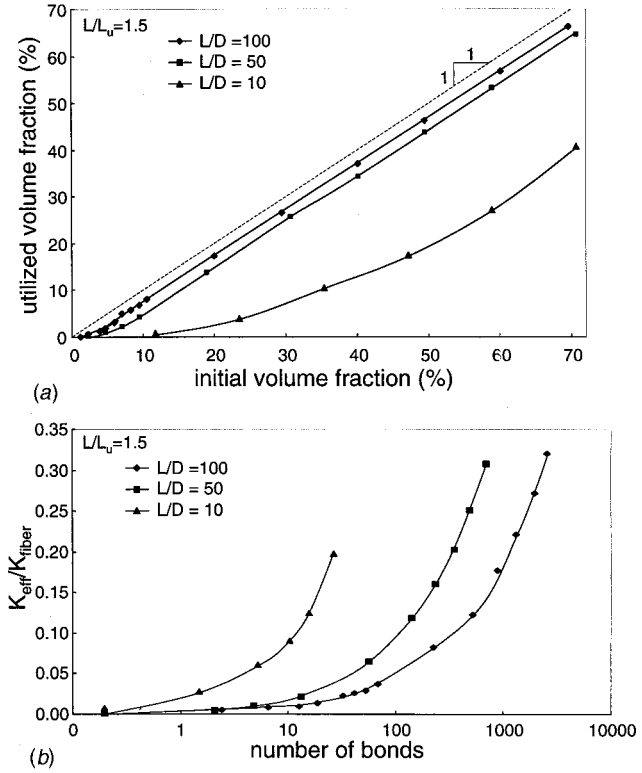

Fig. 4 (*a*) Utilized volume fraction versus original volume fraction, and (*b*) number of bonds, for various aspect ratios, for the case where the staple length is 1.5 × unit cell length. Twenty simulations were performed for each case; averaged data are shown.

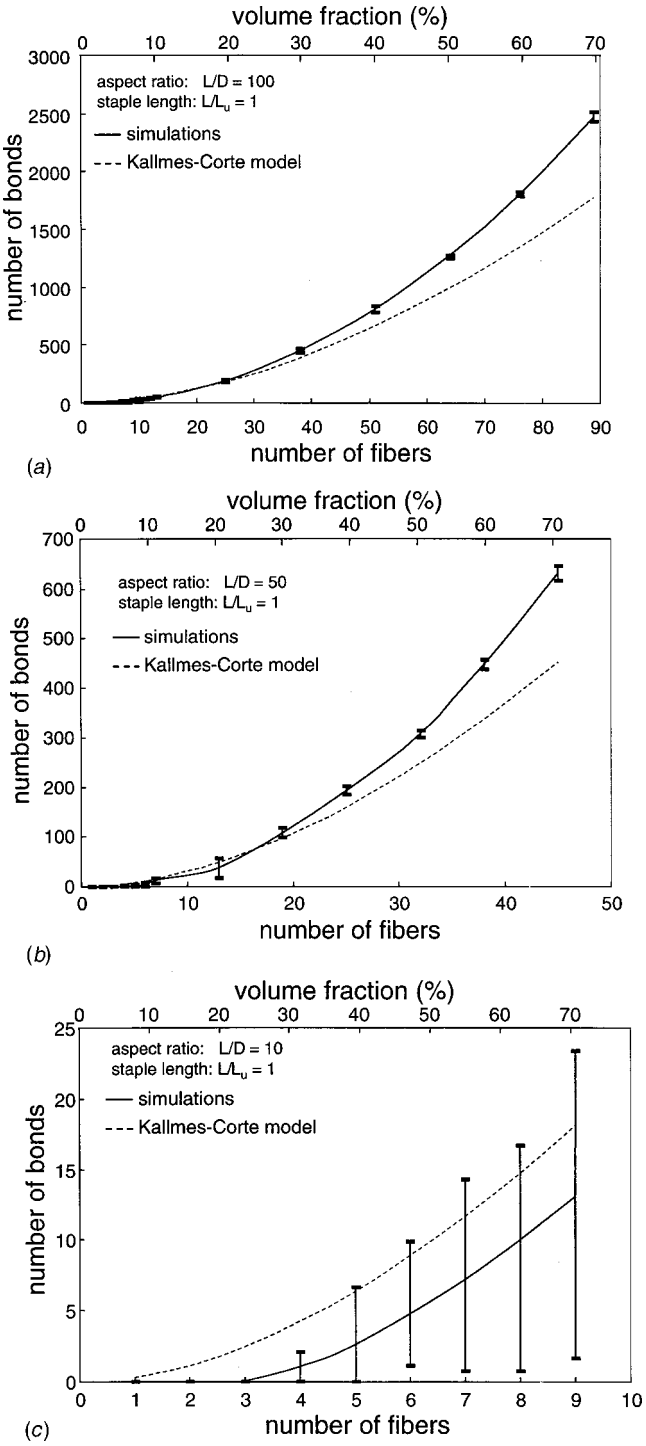

Fig. 5 Number of bonds versus volume fraction—simulations using the present network generation approach versus the theoretical prediction of Kallmes and Corte [8]. Results are shown for three aspect ratios of fibers, (*a*) $L/D=100$; (*b*) $L/D=50$, and (*c*) $L/D=10$. In each case, 10 simulations were performed, and results shown are $\pm 1\sigma$.

$=1.5$); these plots are provided to demonstrate robustness of results (i.e., lack of strong scale effect) in a regime typical of Ni/MH substrate materials.

The utilized volume fraction assessment offers a means of evaluating how much material is ''wasted,'' in the sense that a network is designed either to transmit current or bear load. It is important to identify how much added mass improves connectivity, as well as conductivity, versus added mass which simply contributes to nonconducting ''ends'' of the network. Even for the conservative method chosen, where only fiber segments carrying current for unidirectional flow are preserved, the utilized volume fractions are quite close to initial at moderate-to-high volume fractions for aspect ratios greater than around 50 (Figs. 3(*a*) and 4(*a*)). For aspect ratios around 10, however, these utilized fractions are quite low (less than one half) compared to the initial volume fraction, even at moderately high volume fractions of around 50%. In all materials, however, utilized volume fraction represents only a small fraction of initial volume fraction at low density (volume fractions less than around 10%). This result suggests one of two approaches to estimate conductivity, described later.

The highly nonlinear dependence (note the log scale of the abscissa) of conductivity on bond density is seen in Figs. 3(*b*) and 4(*b*). Again, the lower aspect ratio material ($L/D=10$) is much slower to ''percolate;'' averaged data are shown so that families of curves can be compared, but variance in these values is quite high. Bond density, or number of bonds for a given number of fibers, is an important indication of network connectivity.

The closed-form result described earlier [8] as given in Eq. (3), based on a nonperiodic structure, is compared to number of bonds for the periodic approach here, in Fig. 5, for three aspect ratios (100, 50, and 10). Note that despite the network reduction for unidirectional current in all cases, the number of bonds is unaffected in the simulation results: only segments or portions of segments connecting the network to the sides parallel to the current direction were removed; all bonds, however, were preserved. As shown, the closed-form (nonperiodic) model results in predictions of number of bonds well above those in the simulations, for low volume fractions. This overprediction is quite severe for lower

aspect ratios (i.e., comparison of Figs. 5(*a*) and 5(*c*)) shows less correlation between the model and simulations at lower volume fractions). This situation is reversed at higher volume fractions for the two higher aspect ratio cases ($L/D=100$ and $L/D=50$, as in Figs. 5(*a*) and 5(*b*)): simulations predict higher bond density than the closed-form result. Generally, variance in bond number is very high, and as one would expect, much higher for low aspect ratio fibers.

Conductivity of Network Structures: Two Approaches. The divergence of the simulations from closed-form results, and the high variability exhibited by low-density structures in both bond density and volume utilization suggests two microstructural approaches to predict conductivity and variance in conductivity, as described in the following sections.

Effective Volume Approach. This first technique involved generation of networks according to specific parameters, and then calculation of utilized volume fraction in each case (as in Figs. 3 and 4). This volume fraction was used as the conductor volume fraction in the effective medium, or here, porous medium theory ($\overline{K}$ calculated with $f'=f_u$, and $\overline{K}$ plotted versus $f'=f_i$, per Eq. 7(b)) to generate a conductivity for each simulated (initial) volume fraction. Conductivities were generated for a number of simulations, at a given initial volume fraction. Conductivity is plotted versus initial volume fraction in each case. By performing the statistical geometry simulations separately, the approach allowed prediction of conductivity for a presumably more well-connected microstructure based on the reduced, or utilized, volume fraction. In each case, unidirectional current flow was assumed, amounting to a very conservative estimate of material volume fraction involved in conduction for an ostensibly 2D isotropic stochastic network.

Resistor Network Approach. The second technique involved an exact calculation of network conductivity based on a model of each simulated (reduced) structure as an array of series or parallel-arranged fiber segments. Each segment length was used to scale the resistance of the segment, assuming each had identical resistivity, as

$$R_i=\frac{\rho_f L_i}{A_i}=\frac{L_i}{A_i k_f} \tag{10}$$

where

A_i . . . cross-sectional area of *i*th fiber
L_i . . . length of *i*th fiber
ρ_f . . . resistivity of *i*th fiber
k_f . . . conductivity of the fiber material

Figures 6 illustrate, with the network in Fig. 6(*a*) (shown with periodic conditions enforced, but not reduced) converted to the resistor network shown in Fig. 6(*b*).

This method was compared to Kirkpatrick's postulated relationships, per Eq. (5), with the exponent $t=1.3$ (as suggested by Stauffer [11], and $V_c=4.2$ (as suggested by Balberg and Binenbaum [14,15], among others). This power-law relationship is plotted with the upper bound, and the prediction of porous medium theory (per Eq. (7*b*)) and with simulations, reported $\pm 1\sigma$, in Figs. 7. Comparisons are made for aspect ratios of 100, and a wide range (Fig. 7(*a*)) as well as a magnified range at low volume fraction (Fig. 7(*b*)) are shown.

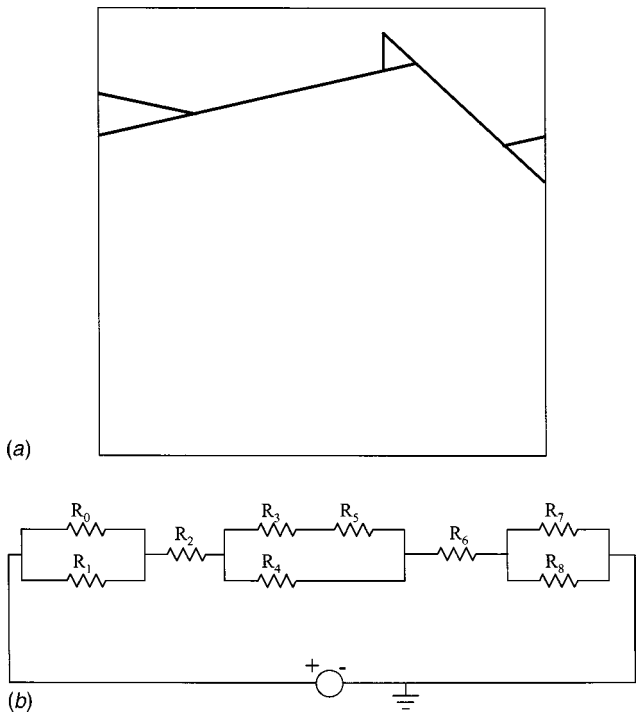

Fig. 6 The resistor network approach (*a*), as in Fig. 4, are used to construct equivalent circuits (*b*)

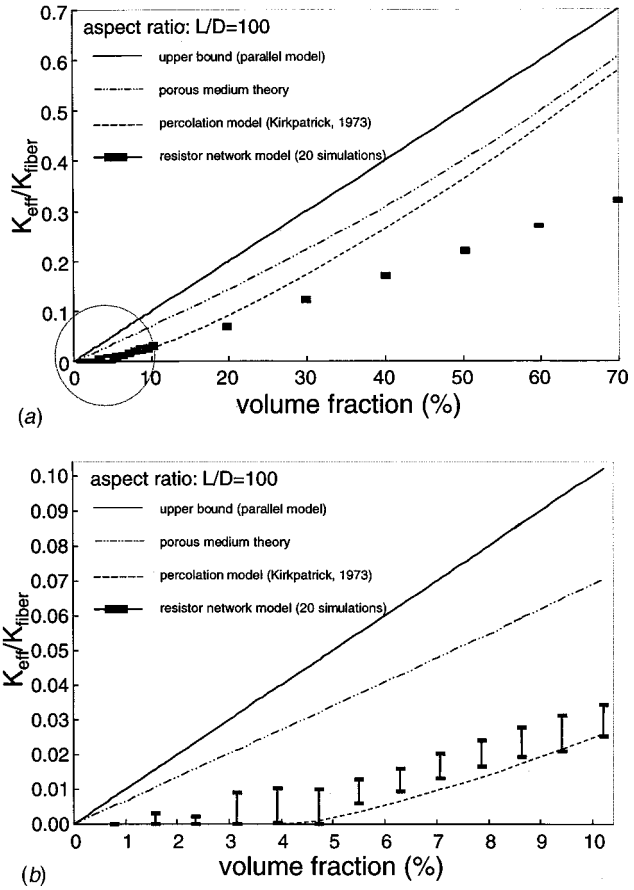

Fig. 7 Comparison of effective conductivities from a classical, semi-empirical percolation approach (after Kirkpatrick [10] using $t=1.3$ per Stauffer [11] and $V_c=4.2$, per Balberg and Binenbaum [14]) with simulation results, the theoretical upper bound (parallel model) and the degenerate result of classical micromechanics; aspect ratios are $L/D=100$ in all cases. Twenty simulations are shown in each case, with error bars denoting $\pm 1\sigma$. A large range is shown in (*a*), with the smaller range of volume fractions enlarged in (*b*).

The semi-empirical approach [10,11] generally underestimates the conductivity of the porous fibrous structures generated, as calculated from an exact resistor network approach. The percolation point for such networks (for aspect ratios ~100) is around 4.2 (this result was confirmed by experimental observations also by Sastry [26]); as such, the percolation model cannot predict conductivities below that point, despite the fact that some of these networks will percolate, although there will be a great deal of variance in properties below the percolation point. Nonetheless, these materials are technologically important for use in substrates, and materials of around 5% volume fraction are commonly used. Given the proximity of these materials' volume fractions to the percolation point, determination of the likely variance in properties in this range is critically important. As shown in Fig. 7(*b*), the percolation model is reasonably accurate in predicting likely percolation, but again, the model predicts deterministically a single-valued conductivity, where the variance is quite high.

III Comparison of Methods

The disparity between the current approach of network generation and predictions of closed-form approaches, and between the prediction of the conductivity using the resistor network approach and the semi-empirical percolation approach or the porous medium theory, have been described. The methods developed here, namely, the ''effective volume approach,'' wherein the network's initial volume fraction of conductive material is corrected to a simulated ''utilized'' volume fraction, and the ''resistor network approach,'' wherein an exact calculation of the network conductivity based on an equivalent series-parallel resistor arrangement to the generated microstructure, are now compared. Figures 8 and 9 show comparisons of each of these two approaches with the porous medium theory (Eq. (7b)), the upper bound (parallel model), the result for two regular lattices (square and hexagonal) and each simulation technique, for $L/D=100$. Figures 8(*a*) and 9(*a*) show comparisons (reported for twenty simulations, each condition, as $\pm 1\sigma$) for the resistor network approach; Figs. 8(*b*) and 9(*b*) give analogous comparisons for the effective volume approach. Plots are given for two aspect ratios (to verify robustness of the technique): $L/L_u=1$ (Fig. 8) and $L/L_u=1.5$ (Fig. 9), respectively. In all cases, variances are quite high. Resistor network calculations, however, show greater variance in properties, with lower overall conductivities, in all cases, than the effective volume simulations.

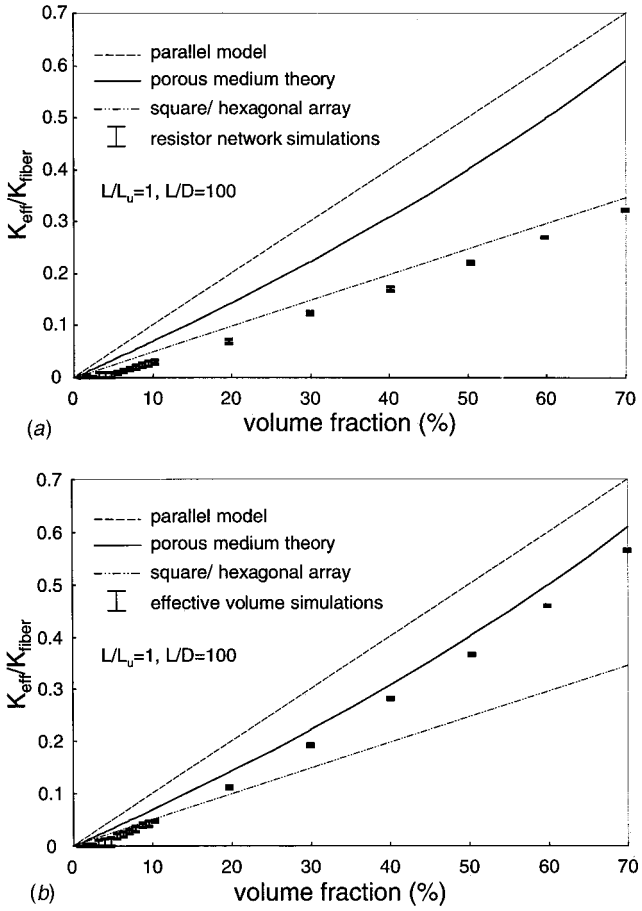

Fig. 8 Simulation ($\pm 1\sigma$) conductivities versus volume fraction, plofted versus the effective medium theory (Eq. (7b)) and the upper (parallel) bound (Eq. 9). Data shown are for $L/L_u=1$, $L/D=100$. Two techniques are shown, including (*a*) the resistor network approach and (*b*) the effective volume approach. Twenty simulations were run for each case.

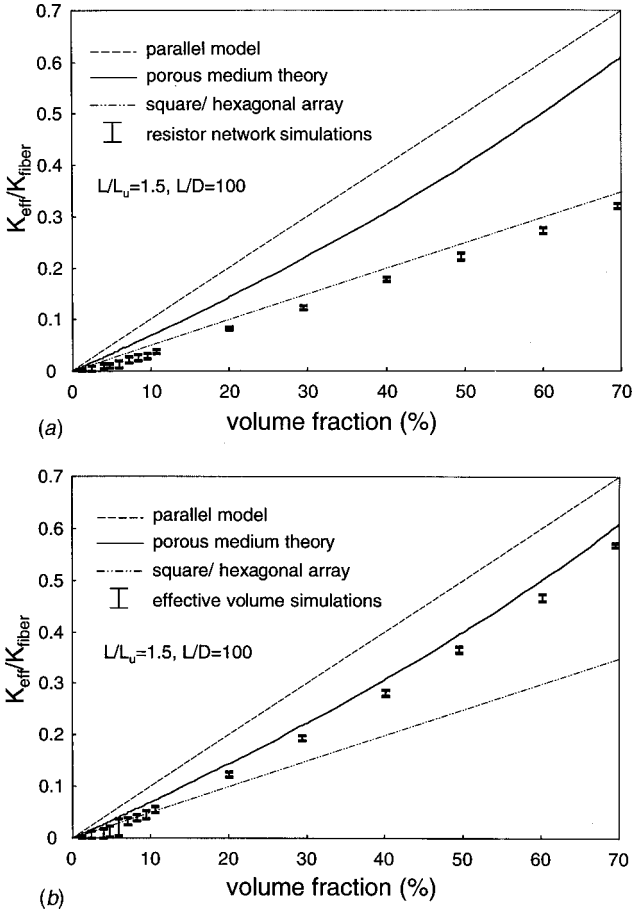

Fig. 9 Simulation ($\pm 1\sigma$) conductivities versus volume fraction, for $L/L_u=1.5$, $L/D=100$, for (*a*) the resistor network approach and (*b*) the effective volume approach. Twenty simulations were run for each case.

IV Comparisons With Experiments

Several materials (Table 1) were tested using an eight-probe resistivity apparatus [1,6,27]. The materials tested in this study were tested in the as-received condition; other work by the present authors has tested these materials in the post-cycled and compressed condition (*ibid.*).

In all cases (Figs. 10), the resistor network approach gives better predictions of both resistivity and variance in resistivity than either the effective volume approach or the porous medium theory. In all cases, the particulate content in the networks was

Table 1 Materials investigated; all produced by National Standard

Material Type	Thickness	Content	Fiber D	Fiber Staple Length	Vol % Nickel
Fibrex *(001-008)*	0.03" (0.075cm)	97% pure nickel, 3% contaminant; 50/50 blend fiber/powder	~30μm	0.25-0.5' (~0.64cm - 1.3cm)	~18%
Fibrex *(001-028)*	0.08" (0.20cm)	97% pure nickel, 3% contaminant; 50/50 blend fiber/powder	~30μm	0.25-0.5' (~0.64cm - 1.3cm)	~7%
AFS *(001-029)*	0.06" (0.15cm)	99.9% pure nickel; 50/50 blend fiber/powder	20μm	0.5-0.75' (~1.3cm - 1.9cm)	~5%
AFS *(001-009)*	0.065" (0.165cm)	99.9% pure nickel; 50/50 blend fiber/powder	20μm	0.5-0.75' (~1.3cm - 1.9cm)	~3%

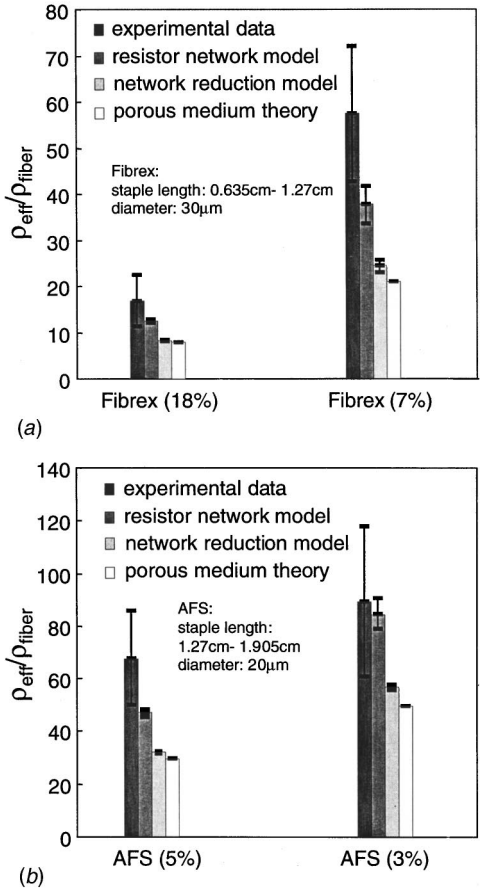

Fig. 10 Experimental data for resistivity versus simulation/model predictions. Two types of material, National Standard Fibrex (7% and 18% by volume) and AFS (3% and 5%) were studied. Each was comprised of a blend of fibers and particles. Simulations were performed for the aspect ratios and staple lengths reported by the manufacturer. Five simulations were run for each case.

considered as fibrous material, thus providing an imperfectly-matched microstructure (more detail on this issue is provided by Cheng and Sastry [28]). However, the predictions were acceptable for the 18% and 5% materials, and the two techniques developed bounded the results for the other two volume fractions (7% and 3%).

V Discussion/Conclusions

Use of these stochastic approaches allows determination of probable connectivities, conductivities and variances in conductivities. Moreover, the predictions differ from those of classical approaches, while allowing direct estimation of variances.

Network Construction/Percolation. A classical closed-form solution for bond density for a network of 1D fibers [9] gives somewhat different results than the numerical approach here. This divergence in predicted bond density can be significant if a semi-empirical percolation model is used [10,11], but again, such a model gives only a single-valued prediction.

The lower prediction, in general, of the network resistor approach with the effective medium approach in material conductivity, coupled with the higher predicted variance, suggests that the stochastic construction of the microstructure is an important factor. Even at relatively high volume fractions, in fact, the effective volume approach deviates significantly from the porous medium theory, and exhibits high variance, so that one can conclude that the stochastic nature of such materials should be accounted for even in these cases. Regular architectures of similar (high) volume fractions would offer much improved performance (i.e., higher conductivity with low variability); it is in the lower volume fraction regime where disordered structures would likely be advantageous.

Use of Regular Lattice Structures. An important question is whether the use of microstructurally-regular lattices (square or hexagonal) is merited, given their typically higher cost. The methods presented here allow detailed comparison of such materials with the stochastic structures of present interest. Longer fibers ($L/D > \sim 100$) must be used if percolation in networks is to be achieved for low densities ($<5\%$ volume fraction); in the case of lower aspect ratio fibers, lattices have a clear and unambiguous advantage for all densities. However, this advantage is markedly less pronounced for volume fractions $>10\%$ in high aspect ratio materials, wherein conductivities are reasonably close to those of perfectly regular lattices. Indeed, the effective-volume simulations predict conductivities exceeding those of the lattices. This technique, however, generally overestimates conductivity (i.e., underestimated resistivity).

Effect of Alignment in Stochastic Structures. The effect of moderate-to-high alignment in these fibrous materials (attendant to many paper-making processes) is a concern if fully 2D conduction is required. The resistor network approach was found to be a superior indicator of both conductivity and variance in conductivity, and was thus used to evaluate this effect (Figs. 11). Networks containing fibers oriented according to normal distributions were generated, with increasing alignment in a single direction. In the first plot shown (Fig. 11(*a*)), conductivity in the direction of alignment is reported; in the second (Fig. 11(*b*)), conductivity in the direction transverse to the direction of alignment is reported. As one would expect, alignment in a particular direction enhances conductivity in that direction (Fig. 11(*a*)). But, interestingly, a very highly aligned network produces a lower conductivity than a

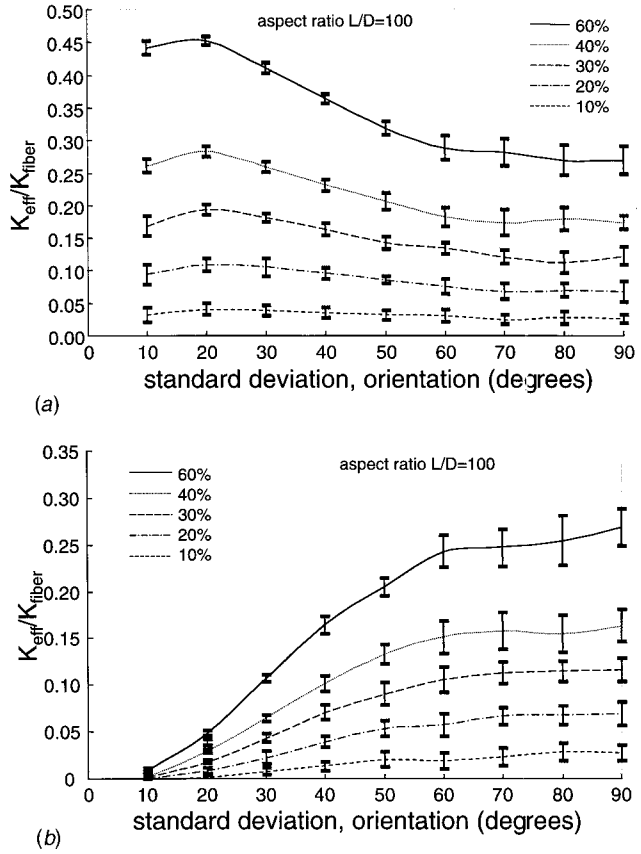

Fig. 11 Evaluation of the effect of alignment in networks, for transverse conductivity. Networks with varying degrees of alignment in the *x*-direction were generated, as shown in (*a*) (here, for a volume fraction ~20%, $L/D=100$, $L/L_u=1$, and average and standard deviation of orientation with respect to the *x*-axis of 0 and 10 deg, respectively). Effective conductivites versus orientation were then calculated via the resistor network approach (as measured by standard deviation of orientation of fibers following a normal distribution for orientation). Twenty simulations were run for each case, and $\pm 1\sigma$ results are shown. (*a*) parallel; (*b*) transverse.

slightly misaligned network in these stochastic networks (compare results at $\sigma_\alpha = 10$ deg versus $\sigma_\alpha = 20$ deg for orientation, α, in Fig. 11(*a*)). This is due to the effect of scale: a slight misalignment causes fiber crossings for lengths on the same order, or less than, the length of the side of the simulation domain. For a highly aligned network, there will be a greater number of fibers which do not span the cell, and thus register as nonconductive. This suggests that alignment studies should be conducted over a large range of sizes, although the general result is likely valid in a real material. The converse situation, wherein conductivity is measured transverse to the direction of alignment, is also important. Figure 11(*b*) gives the results of our calculations (compare with Fig. 11(*a*) for the equivalent fully random networks). For a fairly wide range of alignments, results for transverse conductivity are largely unaffected. Thus, moderate ($\sigma_\alpha > \sim 70$ deg) alignment appears to have little effect on the predictions here.

Future Work. These results suggest that stochastic fibrous networks can be satisfactorily characterized (at least for transport properties) with the simulation techniques described. Closed-form approaches describing both structure and behavior do not adequately describe the variability inherent in these structures. Future work will address the effects of scale in greater detail, particularly differences in scale for mechanics and transport.

Acknowledgments

The authors greatly appreciated support for this research from the Department of Energy and the Lawrence Berkeley Laboratories, under the ETR Program. Additional support from a National Science Foundation PECASE grant is also gratefully acknowledged. Helpful comments from Professor Tom Hales (Mathematics Department, University of Michigan) on various solutions for optimal packing architectures are also acknowledged.

References

[1] Tatarchuk, B. J., 1994, ''Composite Fiber Structures for Catalysts and Electrodes,'' J. Power Sources, **47**, pp. 297–302.
[2] Ferrando, W. A., Lee, W. W., and Sutula, R. A., 1984, ''A Lightweight Nickel Composite Electrode I: Concept and Feasibility,'' J. Power Sources, **12**, No. 3–4, pp. 249–265.
[3] Fritts, D. H., 1981, ''Testing the Mechanical Characteristics of Sintered Nickel Battery Plaque and Their Relationship to Nickel Electrode Performance,'' J. Power Sources, **6**, pp. 171–184.
[4] Oshitani, M., Takayama, T., Takashima, K., and Tsuji, S., 1986, ''A Study on the Swelling of Sintered Nickel Hydroxide Electrodes,'' J. Appl. Electrochem., **16**, pp. 403–412.
[5] Cheng, X., Wang, C. W., Sastry, A. M., and Choi, S. B., 1999, ''Investigation of Failure Processes in Porous Battery Substrates: Part II—Simulation Results and Comparisons,'' ASME J. Eng. Mater. Technol., **121**, No. 4, pp. 514–523.
[6] Wang, C. W., Cheng, X., Sastry, A. M., and Choi, S. B., 1999, ''Investigation of Failure Processes in Porous Battery Substrates: Part I—Experimental Findings,'' ASME J. Eng. Mater. Technol., **121**, No. 4, pp. 503–513.
[7] Broadbent, and Hammersly, 1957, ''Percolation Processes I. Crystals and Mazes,'' Proc. Cambridge Philos. Soc., **53**, pp. 629–641.
[8] Kallmes, O., and Corte, H., 1960, ''The Structure of Paper I. The Statistical Geometry of an Ideal Two Dimensional Fiber Network,'' Tappi J., **43**, No. 9, pp. 737–752.
[9] Corte, H., 1969, ''Statistical Geometry of Random Fiber Networks,'' *Structure, Solid Mechanics and Engineering Design, the Proceedings of the Southampton 1969 Civil Engineering Materials Conference, Part 1*, Te'eni, M., ed., Wiley-Interscience, 1971, pp. 314–355.
[10] Kirkpatrich, 1973, ''Percolation and Conduction,'' Rev. Mod. Phys., **45**, pp. 574–588.
[11] Stauffer, D., 1979, ''Scaling Theory of Percolation Clusters,'' Phys. Rep., Phys. Lett., **54**, No. 1, pp. 1–74.
[12] Pike, G. E., and Seager, C. H., 1974, ''Percolation and Conductivity: A Computer Study. I*,'' Phys. Rev. B, **10**, No. 4, pp. 1421–1434.
[13] Seager, C. H., and Pike, G. E., 1974, ''Percolation and Conductivity: A Computer Study. II*,'' Phys. Rev. B, **10**, No. 4, pp. 1435–1446.
[14] Balberg, I., and Binenbaum, N., 1983, ''Computer Study of the Percolation Threshold in a Two-dimensional Anisotropic System of Conducting Sticks,'' Phys. Rev. B, **28**, No. 7, pp. 3799–3812.
[15] Balberg, I., and Binenbaum, N., 1984, ''Percolation Thresholds in the Three-dimensional Stick System,'' Phys. Rev. Lett., **52**, No. 17, pp. 1465–1468.
[16] Taya, M., and Ueda, N., 1987, ''Prediction of the In-Plane Electrical Conductivity of a Misoriented Short Fiber Composite: Fiber Percolation Model versus Effective Medium Theory,'' ASME J. Eng. Mater. Technol., **109**, pp. 252–256.
[17] Ostoja-Starzewski, M., Sheng, P. Y., and Jasiuk, I., 1994, ''Influence of Random Geometry on Effective Properties and Damage Formation in Composite Materials,'' ASME J. Eng. Mater. Technol., **116**, pp. 384–391.
[18] Ostoja-Starzewski, M., Sheng, P. Y., and Alzebdeh, K., 1996, ''Spring Network Models in Elasticity and Fracture of Composites and Polycrystals,'' Comput. Mater. Sci., **7**, pp. 82–93.
[19] Meredith, R. E., and Tobias, C. W., 1962, ''II. Conduction in Heterogeneous Systems,'' *Advances in Electrochemistry and Electrochemical Engineering*, Interscience, New York, pp. 15–47.
[20] Batchelor, G. K., 1974, ''Transport Properties of Two-Phase Materials with Random Structure,'' Annual Reviews in Fluid Mechanics, **6**, pp. 227–255.
[21] Maxwell, J. C. A, 1891, *Treatise on Electricity and Magnetism I*, Dover, New York.
[22] Hashin, Z., 1962, ''The Elastic Moduli of Heterogeneous Materials,'' ASME J. Appl. Mech., **29**, pp. 143–150.
[23] Christensen, R. M., and Lo, K. H., 1979, ''Solutions for Effective Shear Properties in Three Phase Sphere and Cylinder Models,'' J. Mech. Phys. Solids, **27**, pp. 315–330.
[24] Warren, W. E., and Kraynik, A. M., 1987, ''Foam Mechanics: the Linear Elastic Response of Two-Dimensional Spatially Periodic Cellular Materials,'' Mech. Mater., **6**, pp. 27–37.
[25] Gibson, L. J., 1989, ''Modeling the Mechanics Behavior of Cellular Materials,'' Mater. Sci. Eng., **110**, pp. 1–36.
[26] Sastry, A. M., 1994, ''Modeling Conductivity of Composite Substrates for Nickel-Metal Hydride Batteries,'' Sandia Report SAND94-2884.
[27] Sastry, A. M., Cheng, X., and Choi, S. B., 1998, ''Damage in Composite NiMH Positive Electrodes,'' ASME J. Eng. Mater. Technol., **120**, pp. 280–283.
[28] Cheng, X., and Sastry, A. M., ''On Transport in Stochastic, Heterogeneous Fibrous Domains,'' Mech. Mater., **31**, pp. 765–786.